NIRPS fiber-link design, performances and modal noise mitigation performances tested on sky

Yolanda G. C. Frensch[a,b], François Bouchy[a], Nicolas Blind[a], José Luis Rasilla[c], Frédérique Baron[d], René Doyon[d], Félix Gracia[c], Gaspare Lo Curto[b], Lison Malo[d], and François Wildi[a]

[a]Université de Genève, Chemin Pegasi 51, 1290 Versoix, Switzerland
[b]European Southern Observatory, Alonso de Córdova 3107, Vitacura, Chile
[c]Instituto de Astrofísica de Canarias, Calle Vía Láctea, s/n E-38205, La Laguna, Spain
[d]Université de Montréal, 2900, boul. Édouard-Montpetit, Montréal, H3T 1J4, Canada

ABSTRACT

NIRPS (Near Infra-Red Planet Searcher) is an AO-assisted and fiber-fed high-resolution spectrograph operating in the YJH-bands at the ESO 3.6m telescope in La Silla Observatory, Chile. The optimal geometrical scrambling and the minimization of the modal noise, requested to reach 1 m/s precision in radial velocity, is obtained by combining octagonal fibers, a fiber stretcher, a double-scrambler, and a tip-tilt scanning of the 29-µm fiber core. We tested the performance of the fiber-link design on sky and evaluated the modal noise mitigation via near- and far-field images taken at the fiber-link output. Without the inclusion of the stretcher and tip-tilt scanning, an injection position at the edge of the fiber induces a change in radial velocity of ∼20 m/s with respect to an injection at the center. Observations with the entire instrument of fast-rotating hot stars show that the stretcher and tip-tilt scanning significantly reduce the modal noise from 1.6% to 0.7%. Optimizing the tip-tilt scanning pattern can further minimize the modal noise, thereby improving the precision in radial velocity.

Keywords: NIRPS, Fiber-Link, Modal Noise

1. INTRODUCTION

NIRPS recently joined HARPS (High Accuracy Radial velocity Planet Searcher) at the 3.6m telescope in La Silla. The two spectrographs can be operated simultaneously without degrading the HARPS performance and together cover an unprecedented (precise and wide) wavelength range from 0.37µm to 1.8µm. NIRPS is designed to explore the planetary systems around M dwarfs, aiming for a precision of 1 m/s.[1] To achieve its science goals, NIRPS operates with a spectral resolution of 100 000 in the Y-, J- and H-bands (0.98µm to 1.8µm). Four fibers feed the spectrograph providing two observing modes, a high-accuracy mode (HA) using a 0.4" FoV fiber and a high-efficiency mode (HE) using a 0.9" FoV fiber coupled to a pupil slicer. NIRPS uses a high order adaptive optics (AO) system to couple the starlight into the relatively small (29-µm) multi-modes fiber. From this multi-modes fiber one of the limiting factors in precision arises: the modal noise. In this paper, we describe the on sky performances of the NIRPS fiber-link with its various components that reduce the modal noise and so improve the stability and precision.

2. NIRPS FIBER-LINK

In December 2021, we had the unique opportunity to evaluate the performance of the NIRPS spectrograph fiber-link on sky. We coupled the NIRPS Fiber-Link to the Front-End and tested the AO injection to the HA and HE fibers, while varying the inclusion of the various Fiber-Link sub-components, see Figure 1 for an overview. The Front-End design and performance is described by Blind et al. (this proceeding).[2] Here we will only introduce the relevant Fiber-Link components.

Further author information:
Y.G.C. Frensch: E-mail: jolanda.frensch@eso.org, F. Bouchy: E-mail: françois.bouchy@unige.ch

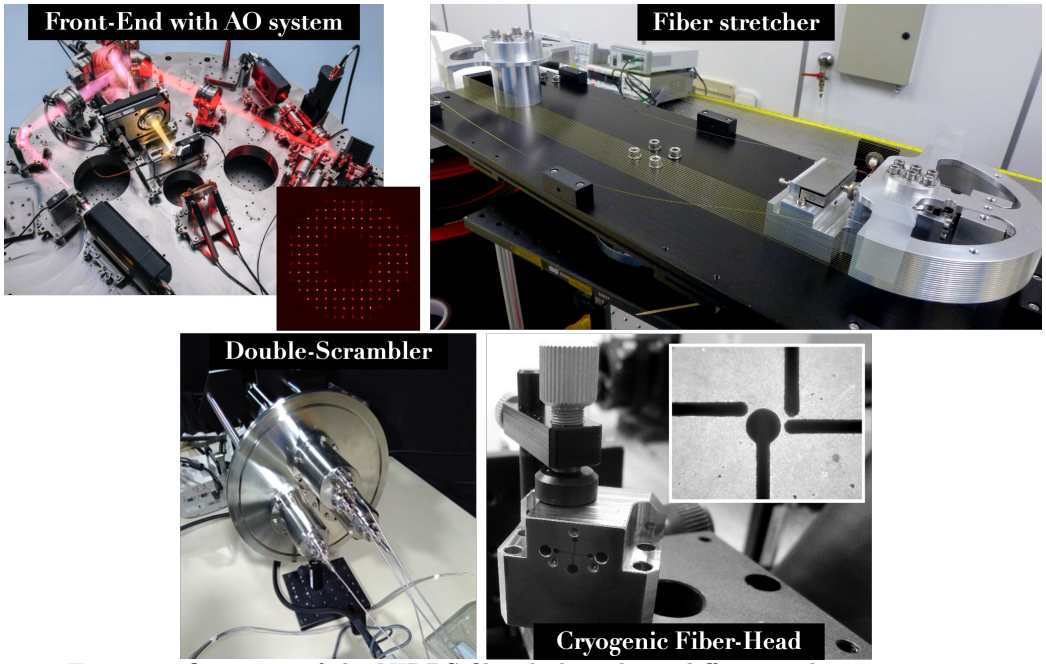

Figure 1: Overview of the NIRPS fiber link with its different sub-components.

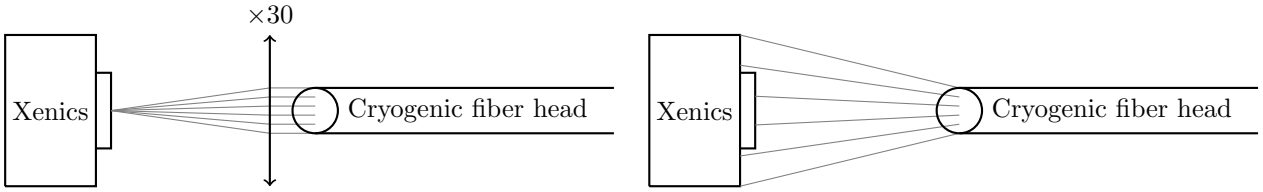

Figure 2: A schematic overview of the fiber-link near-field (left) and far-field (right) test setup.

The Front-End AO system[3] includes a tip-tilt device used for the guiding centering or de-centering and to also offer the possibility to scan the fiber entrance. The stellar beam can be projected into the fiber center, or at the edge of the fiber, and can also sweep the fibre core using different scanning pattern and scanning amplitude. The fiber sections are octagonal to improve the scrambling of the spatial modes inside the fibres as described by Bouchy et al. (2013)[4] and Lo Curto et al. (2015).[5] As an octagonal fiber only scrambles the geometry of the near-field (stellar image), the near- and far-field are exchanged by the double-scrambler and re-injected into an octagonal fiber to also scramble the far-field. The geometry of the output at the exit of the fiber should therefore be uniform and stable if not limited by the modal noise. To minimize the impact of the modal noise, the small HA fiber is physically stretched with piezos at a frequency of 0.3 Hz, which modulates the path length of the light.The second approach to minimize the modal noise is to use the tip-tilt to sweep and to scan uniformly all the propagation modes of the fiber entrance.

To quantify the impact of both the stretcher and the tip-tilt scanning mode, we re-imaged the cryogenic fiber head on a Xenics-Xeva camera (520x640 pixels of 20 µm) using a total magnification of 30x, as visible in Figure 2. During the night the light source was star light and during the day a 1.55 µm laser, both are unfiltered. Both modes (HA and HE) of the science fiber are positioned in the Xenics image, reducing the needed setup changes to a minimum. For the far-field images, the magnification lens was removed and the Xenics camera was moved to a distance of about 33 mm. To prevent the dark noise from dominating, we combined several exposures with a maximum exposure time of 0.3 seconds.

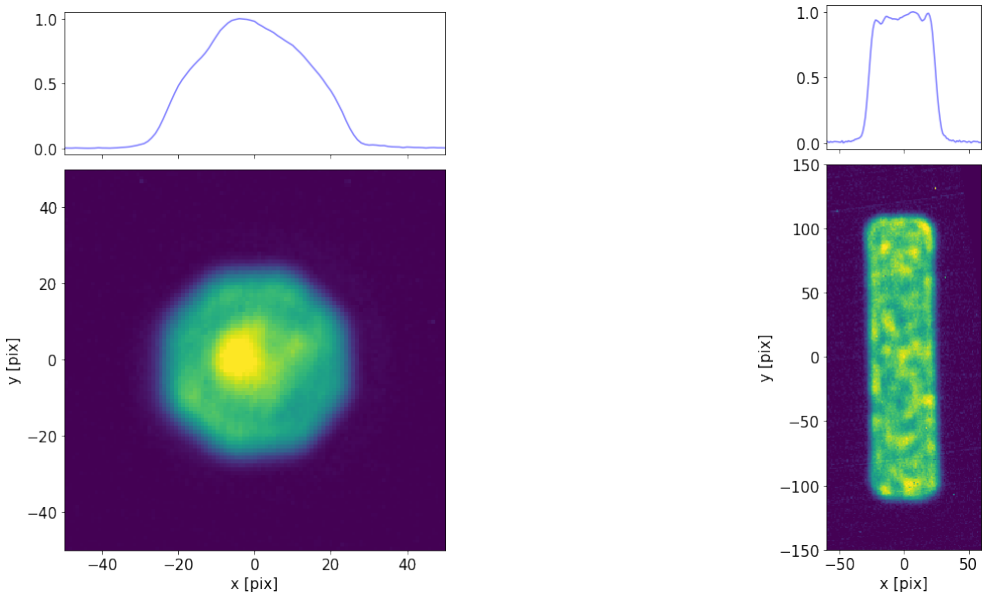

Figure 3: Near-Field Images of the 29-µm octagonal HA fiber (Left) and the 33x132 µm rectangular HE fiber (Right) illuminated with a 1.55 µm laser and the diffraction limited PSF of the Front-End. The y-axis integrated flux is plotted at the corresponding axis.

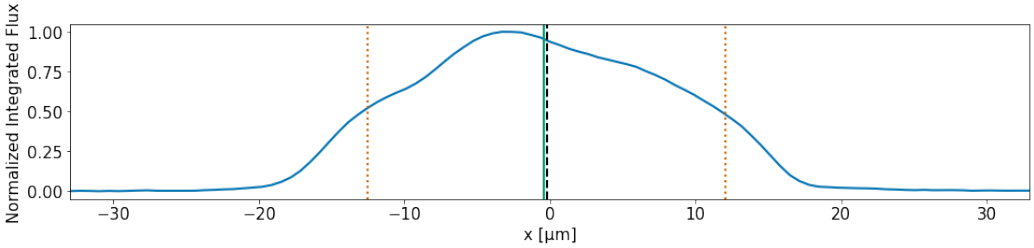

Figure 4: The average integrated flux on the main dispersion axis (y-axis) of the HA Near-Field (see also Figure 3). The red dotted lines are the fiber edges as defined by the maximum of the differential. The dashed black line is the center of the fiber edges. The green solid line is the gravitational center.

3. DATA ANALYSIS

All images are corrected for the flat field and dark (corresponding in exposure time). The far-field images are windowed by a circular mask with a radius of 200 pixels, the HA near-field images by 50 × 50 pixels and the HE near-field by 60 × 150 pixels. Before windowing the HE near-field rectangular images are rotated by -8 degrees to be aligned with the detector columns. In figure 3 near-field images of the HA and HE fiber are visible. The stretcher and tip-tilt scanning are off, the source is unfiltered laser light (1.55 µm) and the width is corrected for the magnification. The modal noise is clearly visible.

The normalized integrated flux projected on the main dispersion (vertical) axis is also shown. The integrated flux is used to determine the centroid of the near-field fiber output, in order to estimate the impact on the apparent radial velocity shift. The centroid is defined as the weighted average with respect to the fiber edges in order to take into account any instability of our optical set-up. First the edges of the fiber are found by the differential maximum of the integrated flux (red dotted lines in Figure 4). If the fiber output is evenly distributed, the centroid is in the middle of the fiber edges. The middle of the fiber edges is therefore used as the reference point (black dashed line in Figure 4). Second the center of gravity is derived by the weighted average, using the integrated flux as weights (green solid line in Figure 4).

Various sequences were performed, varying the inclusion of the fiber stretcher and tip-tilt scanning. For these various sequences we calculated the center of gravity with respect to the fiber edges for all individual images.

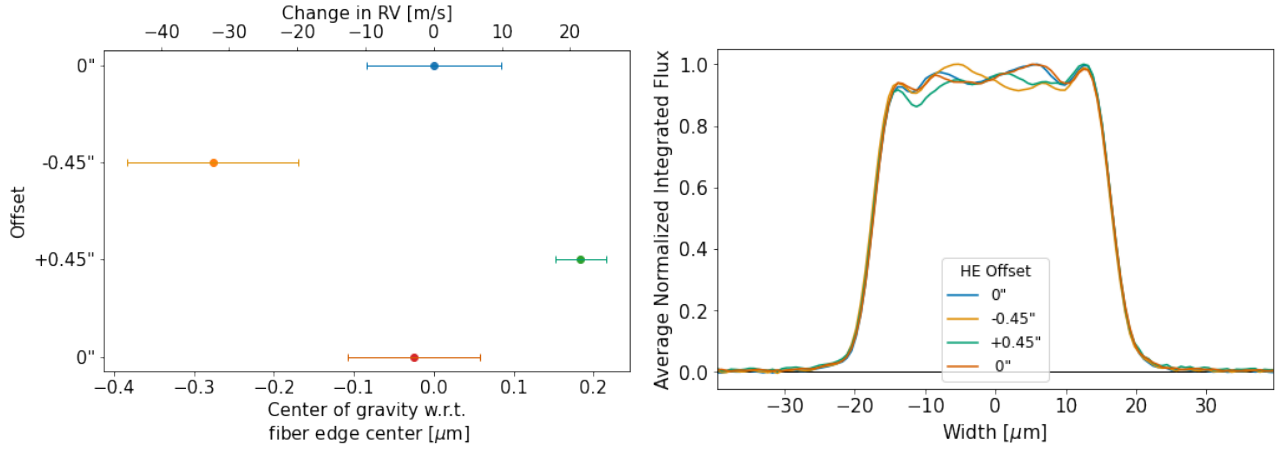

(a) The change in position of the centroid. (b) Integrated flux on the main dispersion axis.

Figure 5: The HE Near-Field, where the injection positions are differed between the center and the edge of the fiber (±0.45").

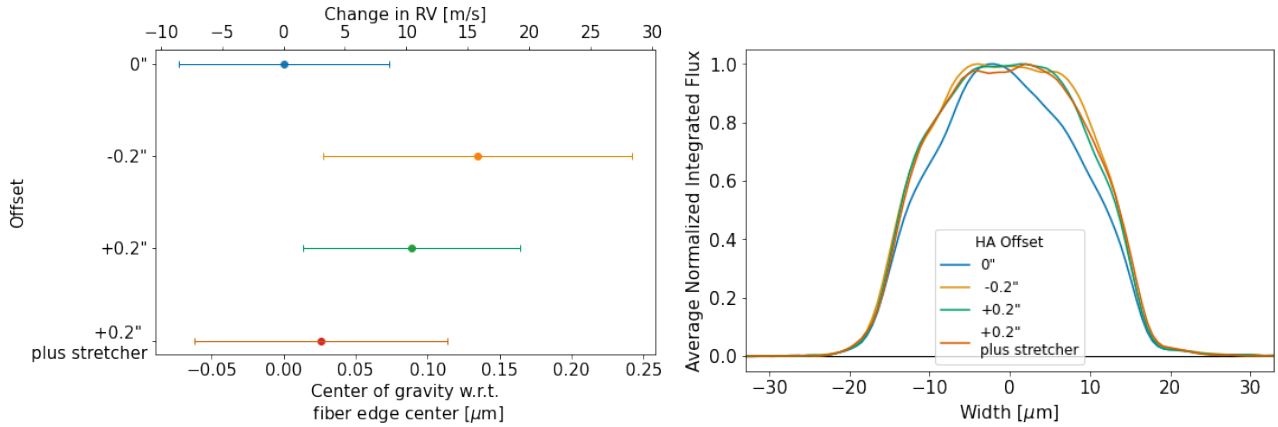

(a) The change in position of the centroid. (b) Integrated flux on the main dispersion axis.

Figure 6: The HA Near-Field, where the injection positions are differed between the center and the edge of the fiber (±0.2") and one including the fiber stretcher.

As the tip-tilt scanning and stretcher impact is only visible over longer timescales the images are then averaged and the error is defined by the standard deviation.

Figure 5a shows a sequence with laser light (1.55 μm), without a stretcher or tip-tilt scanning. The injection position is changed from the center to the edge (±0.45") and then back to the center of the HE fiber. The first sequence is set to zero as a reference point. Injections at the edge create a change in RV of -30 m/s and 20 m/s. Then bringing the injection back to the center also brings the center of gravity with respect to the fiber edge back to it's initial position. **The injection position induces a change in RV of ±20 m/s at the edge of the fiber.** Considering that the guiding accuracy with the tip-tilt is at the level of 0.01", the impact on the radial velocity should not be larger than 1 m/s. Figure 5b shows the corresponding integrated flux. Each point and average flux are 50 images with an exposure time of 0.3 seconds combined.

Figure 6a shows a similar sequence done in HA, allowing us to include the fiber stretcher. Again the injection position at the edge induces a change in RV, this time in the order of 15 m/s. **The fiber stretcher significantly reduces the change in RV back to a position in the order of 'no offset'.** Figure 6b shows the corresponding integrated flux. Here it's visible that the stretcher evens out the profile. Again, each point and average flux are 50 images with an exposure time of 0.3 seconds combined.

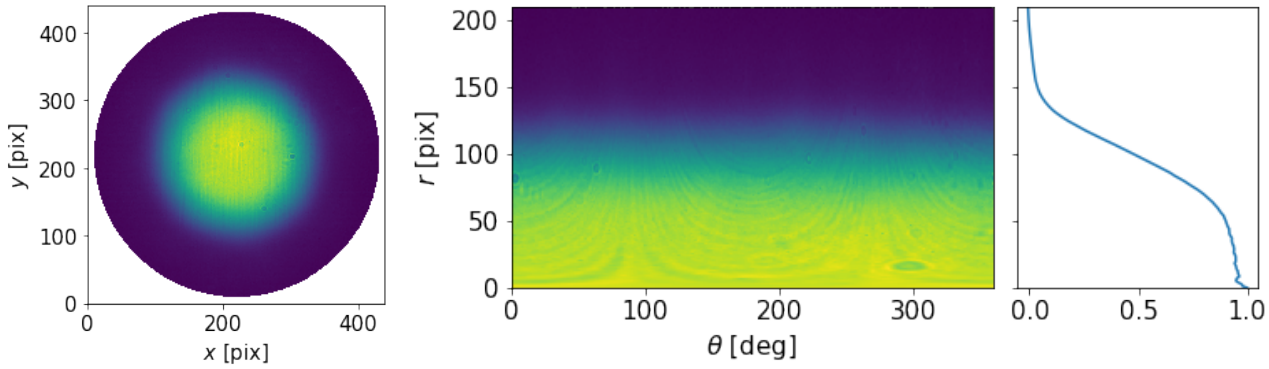

Figure 7: Far-field image of the 29-µm octagonal HA fiber in cartesian coordinates (left) and in polar coordinates with the integrated flux (right).

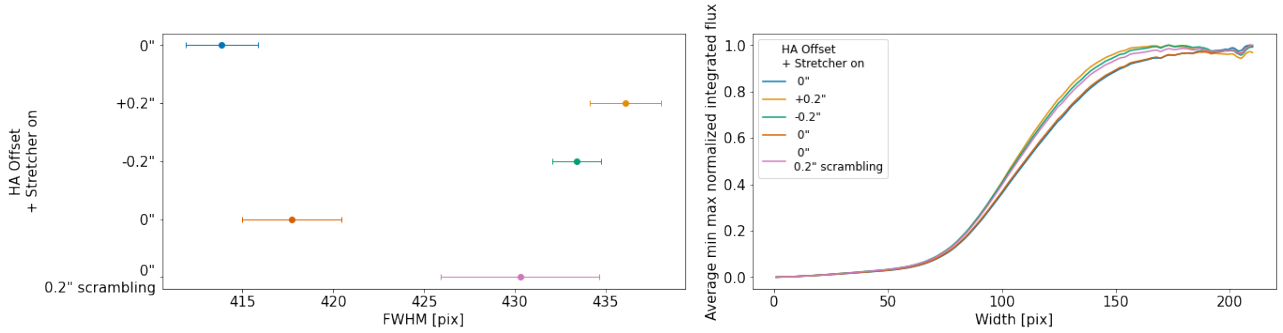

(a) The change in FWHM.

(b) Integrated flux over θ.

Figure 8: The HA Far-Field sequences, where the injection positions are varied between the center and the edge of the fiber (±0.2”). Here scrambling means tip-tilt scanning with an annular of 0.3”. The stretcher is on for all sequences.

For the far-field sequences (see example in Figure 7) we looked at the full-width at half-maximum (FWHM) of the average normalized integrated flux, summed over θ in polar coordinates. All sequences are 50 individual images combined, for HE the exposure time was 0.2 seconds and for HA the exposure time was 0.3 seconds. Figure 9 shows the FWHM as a function of the injection position. A change in illumination is again visible for injection at the edge (±0.45” for HE and ±0.2” for HA). Such change in the Far-Field is directly propagated to the echelle grating illumination. Impact on RV depends on the image quality of the grating and cannot be directly estimated.

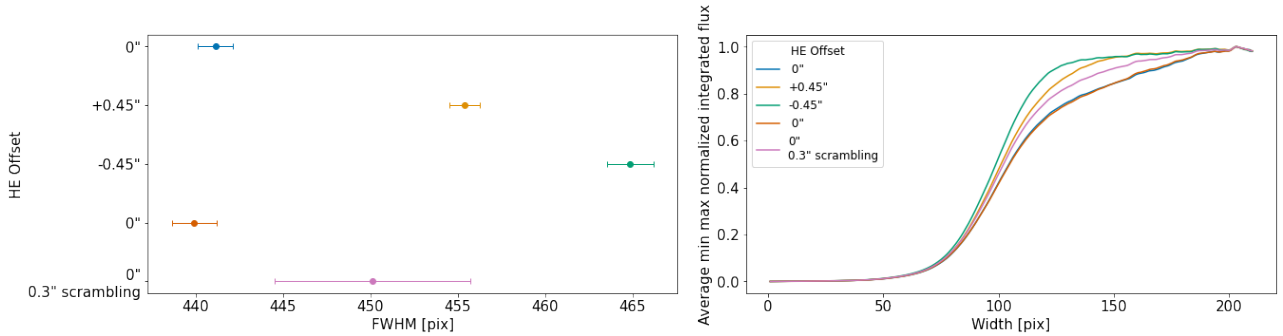

Figure 9: The HE Far-Field sequences, where the injection positions are varied between the center and the edge of the fiber (±0.45”). Here scrambling means tip-tilt scanning with an annular of 0.3”.

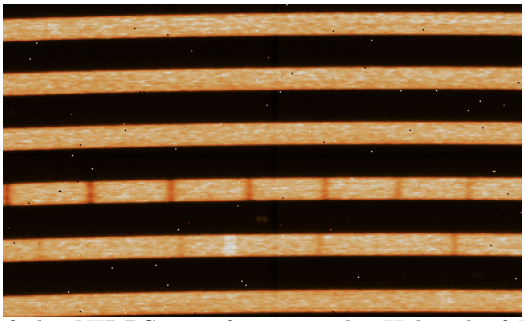

Figure 10: Zoom on a portion of the NIRPS raw frame in the H band of HD195094 observed in HE mode illustrating modal noise. The few spectral features correspond to telluric lines.

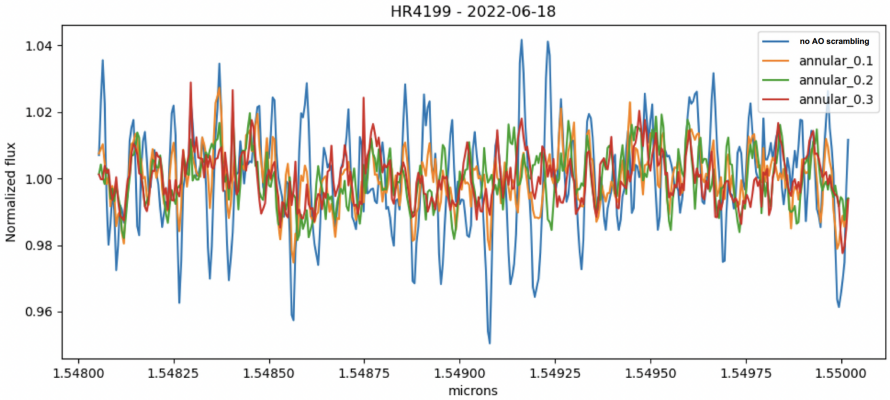

Figure 11: Portion of HA extracted spectrum of the fast rotating hot star HR4199 in the H-band (1.55 µm).

The stretcher is not expected to play a role for the far-field images. The tip-tilt scanning should have an intermediate FWHM, as the scanning injects light both at the center and at the edge of the fiber. **From the far-field images we can again see the fiber injection position induces a change, this time in the illumination, the stretcher does not have impact on the far-field, the tip-tilt scanning (scrambling) results in an intermediate FWHM (as expected).**

4. TESTS WITH NIRPS SPECTROGRAPH

In June 2022, the first commissioning with the entire instrument took place and NIRPS had its first light. We investigated the modal noise properties by observing fast-rotating hot stars. Clear structures at the 0.5-2% level appear in the continuum of stellar spectra after spectral flat-field correction, especially in the H band. See also Figure 10

We investigated the amplitude of the modal noise by measuring the dispersion on the continuum of feature-less spectra. The fiber stretcher clearly shows a significant improvement reducing the modal noise by a factor ∼5. The tip-tilt scanning of the fiber entrance with the AO system also allows to significantly reduce modal noise by filling-up homogeneously as many modes as possible.

If AO injects a corrected image (close to diffraction limit) in the center of the fiber core (no AO scrambling), modal noise reaches about 1.6% for the HA fiber. As expected, scanning the fiber entrance with tip-tilt reduces modal noise, and we observe that an annular scanning between 0.1" and 0.3" (avoiding central modes) significantly reduced the modal noise from 1.6% to 0.7%. An optimum tip-tilt scanning can still be defined in order to minimize the modal noise without significant coupling loss. Furthermore we identified that fact that residual structures of the modal noise are stable over few hours, and independent of, e.g., the telescope pointing.

5. CONCLUSIONS

Fiber modal noise could be a severe limitation for nIR spectroscopy. Both NIRPS fiber stretcher and NIRPS tip-tilt scanning have demonstrated their efficiency on-sky to significantly reduce the modal noise. The AO scanning pattern can still be optimized to minimize the modal noise. Residual quasi-static modal noise can also be calibrated on fast-rotating hot stars since the structure seems relatively stable with time.

In the near future to minimize the modal noise even more, we will try to defocus the AO, shake the fiber that is going towards the calibration unit in order to remove speckles that might already be present there, and optimize the tip-tilt AO scanning pattern.

ACKNOWLEDGMENTS

?

REFERENCES

[1] Bouchy, F., Doyon, R., Artigau, , Melo, C., Hernandez, O., Wildi, F., Delfosse, X., Lovis, C., Figueira, P., Canto Martins, B. L. ., González Hernández, J. I. ., Thibault, S., Reshetov, V., Pepe, F., Santos, N. C., de Medeiros, J. R. ., Rebolo, R., Abreu, M., Adibekyan, V. Z., Bandy, T., Benz, W., Blind, N., Bohlender, D., Boisse, I., Bovay, S., Broeg, C., Brousseau, D., Cabral, A., Chazelas, B., Cloutier, R., Coelho, J., Conod, U., Cumming, A., Delabre, B., Genolet, L., Hagelberg, J., Jayawardhana, R., Käufl, H. U., Lafrenière, D., de Castro Leão, I. ., Malo, L., de Medeiros Martins, A. ., Matthews, J. M., Metchev, S., Oshagh, M., Ouellet, M., Parro, V. C., Rasilla Piñeiro, J. L. ., Santos, P., Sarajlic, M., Segovia, A., Sordet, M., Udry, S., Valencia, D., Vallée, P., Venn, K., Wade, G. A., and Saddlemyer, L., "Near-InfraRed Planet Searcher to Join HARPS on the ESO 3.6-metre Telescope," *The Messenger* **169**, 21–27 (9 2017).

[2] Blind, N., Conod, U., de Meideros, A., Wildi, F., Bouchy, F., Bovay, S., Brousseau, D., Cabral, A., Genolet, L., Kolb, J., Schnell, R., Segovia, A., Sordet, M., Thibault, S., Wehbe, B., and Zins, G., "NIRPS Front-End: Design, performance, and lessons learned," **This proceeding** (2022).

[3] Blind, N., Conod, U., and Wildi, F., "Few-mode fibers and AO-assisted high resolution spectroscopy: coupling efficiency and modal noise mitigation," (11 2017).

[4] Bouchy, F., Díaz, R. F., Hébrard, G., Arnold, L., Boisse, I., Delfosse, X., Perruchot, S., and Santerne, A., "SOPHIE+: First results of an octagonal-section fiber for high-precision radial velocity measurements," *Astronomy & Astrophysics* **549**, A49 (1 2013).

[5] Lo Curto, G., Pepe, F., Avila, G., Boffin, H., Bovay, S., Chazelas, B., Coffinet, A., Fleury, M., Hughes, I., Lovis, C., Maire, C., Manescau, A., Pasquini, L., Rihs, S., Sinclaire, P., and Udry, S., "HARPS Gets New Fibres After 12 Years of Operations," *The Messenger* **162**, 9–15 (12 2015).